Published in final edited form as:
Biochemistry. 2008 November 11; 47(45): 11894–11899. doi:10.1021/bi801211t.

Isotope Exchange at Equilibrium Indicates a Steady State Ordered Kinetic Mechanism for Human Sulfotransferase (SULT1A1)†

Eduard Tyapochkin‡, **Paul F. Cook**§,*, and **Guangping Chen**‡,*

‡*Department of Physiological Sciences, Center for Veterinary Health Sciences, Oklahoma State University, Stillwater, OK 74078, United States*

§*Department of Chemistry and Biochemistry, University of Oklahoma, 620 Parrington Oval, Norman, OK 73019, United States*

Abstract

Cytosolic sulfotransferases (SULTs)-catalyzed sulfation regulates bio-signaling molecule biological activities and detoxifies hydroxyl-containing xenobiotics. The universal sulfuryl group donor for SULT-catalyzed sulfation is adenosine 3′-phosphate 5′-phosphosulfate (PAPS). The reaction products are a sulfated product and adenosine 3′, 5′-diphosphate (PAP). Although the kinetics has been reported since the 1980's, SULTs-catalyzed reaction mechanisms remain unclear. Human SULT1A1 catalyzes the sulfation of xenobiotic phenols and has very broad substrate specificity. It has been recognized as one of the most important phase II drug metabolizing enzymes. Understanding of the kinetic mechanism of this isoform is important for the understanding of drug metabolism and xenobiotic detoxification. In this report, we investigated the SULT1A1-catalyzed phenol sulfation mechanism. The SULT1A1-catalyzed reaction was brought to equilibrium varying substrate (1-naphthol) and PAPS initial concentrations. Equilibrium constants were calculated. In addition, substrate/product equilibrium ratio (S_e/P_e) was determined by perturbation of equilibrium, varying S/P ratios and measuring the shift in product amounts. Two isotopic exchanges at equilibrium: [^{14}C]1-naphthol ⇋ [^{14}C]1-naphthyl sulfate, and [^{35}S]PAPS ⇋ [^{35}S]1-naphthyl sulfate were measured. First order kinetics, observed for all the isotopic exchange reactions studied over the entire time scale monitored, indicates that the system was truly at equilibrium prior to adding isotopic pulse. Complete suppression of ^{35}S isotopic exchange rate upon increasing 1-naphthol and 1-naphthyl sulfate in constant ratio, while no suppression of ^{14}C exchange rate was observed upon increasing PAPS and PAP in constant ratio. Data are consistent with a steady-state ordered kinetic mechanism with PAPS and PAP binding to free enzyme.

Sulfotransferases (SULTs) catalyze the sulfation of hydroxyl-containing compounds as shown in Scheme 1 (1-10). The universal sulfuryl group donor for SULT-catalyzed sulfation is adenosine 3′-phosphate 5′-phosphosulfate (PAPS). The reaction products are a sulfated product and adenosine 3′, 5′-diphosphate (PAP).

Studies of SULT catalytic mechanisms began in the early 1980's. However, the kinetic mechanism of the sulfotransferases has not yet been clearly defined. Initial velocity studies of the rat aryl SULT (AST-IV), were consistent with either a rapid equilibrium random Bi Bi mechanism with two dead-end product complexes or an ordered Theorell-Chance mechanism (11). On the other hand, similar studies of the kinetic mechanism of the human SULT1E1 were

†This work was supported in part by NIH grant GM078606 (G.C.)

Address corresponding to: Guangping Chen, Email: guangping.chen@okstate.edu; Phone: 405-744-2349; Fax: 405-744-1112, And Paul Cook, Email: pcook@ou.edu; Fax: 405-325-7182.

consistent with a random Bi Bi mechanism with two dead-end complexes ((12). Earlier kinetic studies of a bile salt SULT from human liver (13), and the insect SULT, retinal dehydratase (14) also suggested a random kinetic mechanism.

Most of the SULTs studied appear to conform to a steady state ordered Bi Bi kinetic mechanism in which PAPS is the leading substrate. Enzymes studied include the STIII from female rats (an ordered or Iso Theorell-Chance mechanism was proposed) (15), the human SULT1A3 (16,17), a rat tyrosyl protein SULT (TPS, microsomal SULT) (18,19), a plant flavonol 3-SULT (20), and a SULT from *Klebsiella* K-36 (21). In addition, careful studies of the mouse estrogen SULT using initial rate studies, complemented by the crystal structure, structural modeling, and site-directed mutagenesis are consistent with an ordered mechanism with PAPS binding first (10,22-30). Studies of a SULT from rhesus monkey liver were also consistent with an ordered Bi Bi mechanism for sulfation of the hepatotoxin glycolithocholate, but with the bile salt (not PAPS) as the lead substrate (31).

Studies of some bacterial SULTs, on the other hand, are suggestive of a ping-pong Bi Bi mechanism (32-35). A hybrid rapid-equilibrium random two-site ping-pong mechanism was proposed for the bacterial SULT, NodST, with the formation of a sulfated NodST intermediate (32). In this mechanism, PAPS and chitobiose bind independently and randomly at two different sites on NodST. The same group studied another bacterial SULT (Stf0) using mass spectrometry, and concluded that it has a rapid-equilibrium random mechanism (36). Studies of the bacterial arylsulfate SULT (ASST), which catalyzes the transfer of the sulfate group from a phenyl sulfate ester to the phenolic accepter suggested a ping-pong mechanism, and site-directed mutagenesis suggested Tyr123 was the residue in the ASST active site that accepts a sulfate for transfer to another phenolic substrate (35).

Kinetic mechanisms for SULTs catalyzed sulfation reactions are still not clear, reported results and conclusions are in contradictory. Human SULT1A1 is one of the most important phase II drug metabolizing enzymes. It has very broad substrate-specificity, high activity toward most phenolic compounds. It is also widely distributed in human tissues. The kinetic mechanism for human SULT1A1 is not well studied. Isotope exchange at equilibrium is an excellent probe of kinetic mechanism along the reaction pathway (37-39). In this work, isotopic exchange at equilibrium is used to probe the proposed kinetic mechanism (Scheme 2) for human SULT1A1. Data are consistent with a steady state ordered kinetic mechanism.

Experimental Procedures

Chemicals

alpha-[^{14}C]1-Naphthol, (55 mCi/mmol) was purchased from American Radiolabeled Chemicals, Inc. [^{35}S]3′-Phosphoadenosine-5′-phosphosulfate, (2.43 Ci/mmol) was purchased from PerkinElmer, Inc., Boston, MA. 1-Naphthol and adenosine 3′, 5′-diphosphate sodium salt (PAP) were purchased from Sigma-Aldrich, while adenosine 3′-phosphate 5′-phosphosulfate, tetralithium salt (PAPS) was purchased from Calbiochem. 1-Naphthyl sulfate, potassium salt was purchased from MP Biomedicals, LLC.

Thin layer Partsil KC 18 F, silica Gel 60 chromatography plates with fluorescent indicator, (20 × 20 cm, 200 ∝m) Whatman® Schleicher & Schuell, were purchased from Sigma-Aldrich. The plates were channeled using razor blades. A channel width of 1 cm was chosen with a groove width between channels of 2 mm. Deionized water was used in all the experiments. All other reagents and chemicals were the highest analytical grade available. Scintillation counting was carried out on a Beckman LS 6500 Multi-Purpose Scintillation Counter.

Enzyme

SULT1A1 (7.5 mg/mL) purified as described previously (40-42) was used in this study.

Measurement of Equilibrium Constant

All the reactions were carried out in closed microcentrifuge tubes (0.5 mL) to avoid evaporation of buffer. The total reaction volume was 50 ∝L to bring the system to equilibrium quickly. SULT1A1 was added to the reaction mixture last to start the reaction and prevent enzyme's deactivation. The time course for attaining equilibrium was first determined. For example, a solution in 50 mM phosphate, pH 6.2, 37°C, containing 20 μM $[1\text{-naphthol}]_0$ (where the subscript zero indicates initial concentration) and 10 μM $[PAPS]_0$, and SULT1A1 was added to the reaction mixture last to initiate the reaction. With 7.5 ∝g SULT1A1, equilibrium was reached within two hours.

Different initial concentrations of PAPS and ^{14}C-labeled 1-naphthol were incubated with in 50 mM phosphate, pH 6.2 at 37°C until equilibrium was attained. The reaction was stopped with 50 ∝L of TRIS base (0.25 M, pH 8.7). In order to separate ^{14}C-labeled 1-naphthol from the product, ^{14}C-labeled 1-naphthyl sulfate, 100 ∝L of chloroform was added to each eppendorff tube, the mixture was vortexed for 30 s, and centrifuged at 9000 *g* for 5 min. The 1-naphthol extracts into the chloroform phase, while 1-naphthyl sulfate remains in the aqueous phase. The chloroform phase was carefully separated from the aqueous phase using a micro-syringe, and then transferred into a scintillation vial containing 4 mL of scintillation cocktail (EcoLite) and counted. The syringe was rinsed with acetone twice between samples. The liquid-liquid extraction with chloroform was repeated twice. The aqueous phase containing product was transferred into a scintillation vial containing 4 mL of scintillation cocktail (EcoLite) and counted.

The ^{14}C-labeled product was monitored until there was no longer any change with time. Once the system appeared to be at equilibrium the same amount of SULT1A1 (7.5 ∝g) was added to the same reaction mixture to see if any additional change in product was observed. If there was no change in product, K_e was calculated according to Eq. 1.

$$K_e = \frac{[P]_e^2}{[S]_e([\mathrm{PAPS}]_0 - [P]_e)} \quad (1)$$

In Eq. 1, $[P]_e = [PAP]_e$ and $[S]_e = [S]_0 - [P]_e$. Equilibrium substrate and product concentrations were determined from calculated specific radioactivities for each experiment as discussed above.

Two types of control were carried out. The first one made use of the same protocol as discussed above, but in the absence of SULT1A1, while the second one was in the absence of PAPS and/or PAP. No significant difference was observed between the two types of control. The cpm of the controls was subtracted from those of the sample (aqueous phase only). All controls and samples were carried out in triplicate; results are given as means ± *SD*.

The $[S]_e/[P]_e$ ratio was determined with $[S]_0$ fixed at 50 ∝M, but with $[PAPS]_0$ in the range of 0–80 ∝M, the same experimental conditions used to measure the initial rate of isotope exchange. Results are shown in Table 1. In addition, the method of equilibrium perturbation (39) was used to determine the equilibrium constant. The reaction was equilibrated using $[(^{14}C)1\text{-naphthol}]_0$ and $[PAPS]_0$ of 20 ∝M and 10 ∝M, respectively. Various concentrations of cold 1-naphthol and 1-naphthyl sulfate, such that the cold reactants were at least one order of magnitude greater than $[(^{14}C)1\text{-naphthol}]_0$ were added to the reaction mixture. The change

in [^{14}C]1-naphthyl sulfate product concentration was monitored using scintillation counter, as discussed above. The equilibrium position was established at the S/P ratio where no change in product occurs (Fig. 1).

Using [^{35}S]PAPS and 1-naphthol, the equilibrium constant was determined as above for reactions using [^{14}C]1-naphthol. However, termination of the reaction and separation of labeled reactant and product was different. The reaction was stopped with 50 ∝L methanol. Channeled silica gel TLC plates were used to separate [^{35}S]PAPS and [^{35}S]1-naphthyl sulfate. The reaction mixture (100 ∝L) was spotted onto a TLC plate using a micropipette in increments of 5 ∝l. The composition of the mobile phase for the TLC studies was determined experimentally by separating non-radioactive PAPS and product 1-naphthyl sulfate 4 mM and 10 mM, respectively, and viewing the spots with 254 nm UV light. [^{35}S]PAPS and [^{35}S]product were best separated using acetonitrile:methanol:acetic acid:water (25:65:5:5). The TLC plates were developed in a closed glass chamber. After [^{35}S]PAPS and [^{35}S]product separation, the dried TLC plates were subjected to autoradiography (24 hrs), and the radioactive spots were transferred into scintillation vials containing 4 mL of scintillation cocktail (EcoLite) to determine the total amounts of [^{35}S]PAPS remaining and [^{35}S]product formed. Equilibrium concentrations and K_e were calculated using similar approach as described in the above sections. Results are shown in Table 2.

Isotope Exchange at Equilibrium

Rates of isotopic exchange at equilibrium were estimated by adding the radiolabeled reactant to the fully equilibrated reaction system containing SULT1A1. The total concentration of radiolabeled pulse was set at a concentration 100-fold lower than the cold reactant concentration to be certain that no change in the chemical equilibrium position occurred upon addition of the pulse, but with sufficient radioactivity to follow the approach to isotopic equilibrium. The formation of the radiolabeled product was monitored as a function of time until there was no longer any change (Fig. 2). The reaction was then stopped with 50 ∝L of TRIS (0.25 M, pH 8.7). The liquid-liquid extraction protocol described above was used to separate labeled substrate and product.

Rates of isotope exchange were calculated according to Eq. 2 (39), where v_{ex} is the initial velocity of isotopic exchange, *A* and *C* are the equilibrium amounts of the exchanging reactant and product, e. g., 1-naphthol and 1-naphthyl sulfate in micromoles, *t* is the time required to reach *f* fraction of isotopic equilibrium in minutes, and *f* is the fraction of isotopic equilibrium achieved at time *t* ($f = [(^{14}C)S]_t/[(^{14}C)S]_e = [(^{14}C)P]_t/[(^{14}C)P]_e$), subscripts t and e indicate time dependent and equilibrium values, respectively).

$$v_{ex} = -\frac{ACln(1-f)}{(A+C)t[\text{enzyme}]} \quad (2)$$

Results

Equilibrium constant

The equilibrium constant, K_e, was determined independently by monitoring approach to equilibrium beginning with $[PAPS]_0$ and $[1\text{-naphtol}]_0$ or by measuring the perturbation from equilibrium. The K_e was measured at different ratios of 1-naphthol/1-naphthyl sulfate and PAPS/1-naphthyl sulfate and monitoring the change in concentration of radiolabel as equilibrium was attained (Fig. 1) (39). The S/P ratio that gives no change in product after addition of the cold reactants is the one that indicates the system is at equilibrium upon addition of substrate. The K_e values measured are consistent using two different separation methods

(Tables 1 and 2), but are more accurately determined using the liquid-liquid extraction with chloroform. The TLC method is intrinsically less accurate and gave larger errors than those obtained using liquid-liquid extraction with chloroform. The average value of K_e used in subsequent experiments is 0.021 ± 0.004 (Table 1).

[^{14}C]1-Naphthol/[^{14}C]1-Naphthyl Sulfate Isotope Exchange at Equilibrium

A time course for approach to isotopic equilibrium for the exchange monitoring the appearance of [^{14}C]1-naphthyl sulfate is shown in Fig. 2A; isotopic equilibrium is achieved within 2 hours in all cases. When $\ln(1 - f)$ was plotted versus time in Fig. 2B (where f is the fraction of the equilibrium concentration of [^{14}C]1-naphthyl sulfate attained at time t), it clearly indicated a first order reaction. All of the first order plots were linear for all the isotopic exchange reactions studied over the entire time scale monitored. All the isotopic exchange rates were directly proportional to the enzyme concentration.

The exchange rate, v_{ex}, was calculated from the data in Fig. 3 using eq. 2. In Figs. 2A and B the concentrations of PAPS and PAP 20 ∝M and 4 ∝M, respectively, giving a $[PAPS]_0/[PAP]_0$ ratio of 5 Maintaining the PAPS/PAP ratio at 5, but increasing the concentrations of the two components, gave a family of curves similar to those shown in Fig. 2B, and a plot of the calculated v_{ex} against the concentration of $PAPS_0$ with $[PAPS]_0/[PAP]_0$ maintained at 5, gave the plot shown in Fig. 3. The plot is hyperbolic and a fit of the data in Fig. 3 to the Michaelis-Menten equation gave a K_{PAPS} for the exchange reaction of 2.1 ± 0.5 μM, similar to the K_{PAPS} value of 1 μM obtained for the chemical reaction, and a V_{max} for the exchange reaction, V_{ex}, of 2.96 ± 0.03 ∝M/min/mg. The hyperbolic nature of the ^{14}C-labeled 1-naphthol to 1-naphthyl sulfate exchange rate indicates a lack of suppression of the exchange as a result of increasing $[PAPS]_0/[PAP]_0$.

[^{35}S]PAPS/[^{35}S]1-Napthyl Sulfate Isotope Exchange at Equilibrium

Experiments similar to those carried out above were also carried out for the PAPS to 1-naphthyl sulfate exchange with ^{35}S as the label. The $[PAPS]_0/[PAP]_0$ concentration pair was fixed at 5:1, and the $[S]_0/[P]_0$ (1-naphthol to 1-naphthyl sulfate) ratio was fixed at 10:1. The v_{ex} was then measured as a function of increasing concentration of 1-naphthol with $[S]_0/[P]_0$ maintained in constant ratio.

The maximal rate of the PAPS to 1-naphthyl sulfate isotopic exchange was about four-fold faster than that of the 1-naphthol to 1-naphthyl sulfate isotopic exchange, and isotopic equilibrium was attained within about thirty minutes for the former compared to one-to-two hours for the latter. All of the first order plots were linear (similar to Fig 2A and B, data not shown). A plot of the v_{ex} against the concentration of PAPS with 1-naphthol to 1-naphthyl sulfate maintained at constant ratio exhibits substrate inhibition with a complete depression of v_{ex} at high concentrations (Fig. 4). When 1-naphthol concentrations reach higher than 1.4 mM (140 ∝M 1-naphthyl sulfate), the exchange rate approaches zero.

Discussion

As it is stated in the introduction, there are three kinetic mechanisms that have been postulated for SULTs catalyzed sulfation reactions, including a random mechanism, and one of two ordered mechanisms, that is, with PAPS and PAP binding to free enzyme or with substrate and sulfated product binding to free enzyme, Scheme 2. Although a ping pong mechanism was postulated, it was only observed for bacterial SULTs.

In the case of a random mechanism (Scheme 2, bottom), all plots of v_{ex} vs. a reactant concentration in constant ratio to a product, are usually hyperbolic, but may exhibit partial

suppression of the rate at high concentrations of the reactant/product pair. In the case of a rapid equilibrium random kinetic mechanism the maximum rates of all of the exchange reactions are equal, since all have the same rate limiting step. However, in the case of an ordered mechanism the exchange rate will be suppressed as the inner reactant/product pair (the pair that binds to the EA and EQ complexes) is increased to infinity. Thus, in the case of the ordered mechanism shown at the top of Scheme 2, increasing the 1-naphthol/1-naphthyl sulfate pair will suppress the rate of exchange between PAPS and PAP, or PAPS and 1-naphthyl sulfate. For the ordered mechanism shown in the middle of Scheme 2, increasing the PAPS/PAP pair will decrease the rate of exchange between 1-naphthol and 1-naphthyl sulfate, or PAPS and 1-naphthyl sulfate.

As shown in Figs. 4 and 5, the rate of ^{14}C exchange between 1-naphthol and 1-naphthyl sulfate is not suppressed by increasing PAPS and PAP in constant ratio, but the rate of the ^{35}S exchange between PAPS and 1-naphthyl sulfate is completely suppressed at high concentrations of 1-naphthol and 1-naphthyl sulfate. Data are consistent with the ordered mechanism shown at the top of Scheme 2. The enzyme forms to which 1-naphthol and 1-naphthyl sulfate bind are E:PAPS and E:PAP, and thus increasing PAPS and PAP will increase the concentration of the two enzyme forms the exchanging pair bind to, and thus the exchange rate will be increased. However, PAPS binds to E and 1-naphthyl sulfate binds to E:PAP, and thus increasing 1-naphthol to infinity will trap PAPS on enzyme, and decrease the exchange rate. An increase in the concentration of 1-naphthyl sulfate will increase the production of E:PAPS, but this will still not overcome the effect of increased 1-naphthol concentrations, which prevent release of PAPS. Thus, the mechanism of SULT1A1 is ordered with PAPS and PAP binding to free enzyme.

In this work, we studied human SULT1A1 kinetic mechanism. Other SULTs such as human SULT1A3 and rat SULT1A1 (AST-IV) have very similar kinetic properties as the human SULT1A1. A common kinetic characteristics for almost all cytosolic SULTs is that they show substrate-inhibition. All the SULTs also share the same sulfuryl group donor, PAPS. The kinetic mechanism for the human SULT1A1 may also be applied to other SULTs. Human SULT1A1 has been recognized as one of the most important phase II drug metabolizing enzymes. Understanding of the kinetic mechanism of this isoform is important for the understanding of drug metabolism and xenobiotic detoxification.

Abbreviations

SULT
: sulfotransferase

SULT1A1
: simple phenol sulfotransferase

PAPS
: adenosine 3′-phosphate 5′-phosphosulfate

PAP
: adenosine 3′, 5′-diphosphate

TLC
: thin layer chromatography

References

1. Wang LQ, James MO. Inhibition of sulfotransferases by xenobiotics. Curr Drug Metab 2006;7:83–104. [PubMed: 16454694]

2. Nimmagadda D, Cherala G, Ghatta S. Cytosolic sulfotransferases. Indian J Exp Biol 2006;44:171–182. [PubMed: 16538854]
3. Gamage N, Barnett A, Hempel N, Duggleby RG, Windmill KF, Martin JL, McManus ME. Human sulfotransferases and their role in chemical metabolism. Toxicol Sci 2006;90:5–22. [PubMed: 16322073]
4. Runge-Morris M, Kocarek TA. Regulation of sulfotransferases by xenobiotic receptors. Curr Drug Metab 2005;6:299–307. [PubMed: 16101570]
5. Pacifici GM. Inhibition of human liver and duodenum sulfotransferases by drugs and dietary chemicals: a review of the literature. Int J Clin Pharmacol Ther 2004;42:488–495. [PubMed: 15487807]
6. Chapman E, Best MD, Hanson SR, Wong CH. Sulfotransferases: structure, mechanism, biological activity, inhibition, and synthetic utility. Angew Chem Int Ed Engl 2004;43:3526–3548. [PubMed: 15293241]
7. Coughtrie MW. Sulfation through the looking glass--recent advances in sulfotransferase research for the curious. Pharmacogenomics J 2002;2:297–308. [PubMed: 12439736]
8. Duffel MW, Marshal AD, McPhie P, Sharma V, Jakoby WB. Enzymatic aspects of the phenol (aryl) sulfotransferases. Drug Metab Rev 2001;33:369–395. [PubMed: 11768773]
9. Glatt H, Engelke CE, Pabel U, Teubner W, Jones AL, Coughtrie MW, Andrae U, Falany CN, Meinl W. Sulfotransferases: genetics and role in toxicology. Toxicology Letters 2000;112-113:341–348. [PubMed: 10720750]
10. Negishi M, Pedersen LG, Petrotchenko E, Shevtsov S, Gorokhov A, Kakuta Y, Pedersen LC. Structure and function of sulfotransferases. Archives of Biochemistry & Biophysics 2001;390:149–157. [PubMed: 11396917]
11. Duffel MW, Jakoby WB. On the mechanism of aryl sulfotransferase. Journal of Biological Chemistry 1981;256:11123–11127. [PubMed: 6945304]
12. Zhang H, Varlamova O, Vargas FM, Falany CN, Leyh TS, Varmalova O. Sulfuryl transfer: the catalytic mechanism of human estrogen sulfotransferase. J Biol Chem 1998;273:10888–10892. [PubMed: 9556564]
13. Chen LJ, Segel IH. Purification and characterization of bile salt sulfotransferase from human liver. Archives of Biochemistry & Biophysics 1985;241:371–379. [PubMed: 3862362]
14. Vakiani E, Luz JG, Buck J. Substrate specificity and kinetic mechanism of the insect sulfotransferase, retinol dehydratase. Journal of Biological Chemistry 1998;273:35381–35387. [PubMed: 9857081]
15. Singer SS, Bruns L. Enzymatic sulfation of steroids. XI. The extensive purification and some properties of hepatic sulfotransferase III from female rats. Canadian Journal of Biochemistry 1980;58:660–666. [PubMed: 6936065]
16. Whittemore RM, Pearce LB, Roth JA. Purification and kinetic characterization of a dopamine-sulfating form of phenol sulfotransferase from human brain. Biochemistry 1985;24:2477–2482. [PubMed: 3860259]
17. Whittemore RM, Pearce LB, Roth JA. Purification and kinetic characterization of a phenol-sulfating form of phenol sulfotransferase from human brain. Archives of Biochemistry & Biophysics 1986;249:464–471. [PubMed: 3463246]
18. Vargas F, Frerot O, Brion F, Trung Tuong MD, Lafitte A, Gulat-Marnay C. 3′-Phosphoadenosine 5′-phosphosulfate biosynthesis and the sulfation of cholecystokinin by the tyrosylprotein-sulfotransferase in rat brain tissue. Chemico-Biological Interactions 1994;92:281–291. [PubMed: 8033261]
19. Frerot O, Vargas F. Cholecystokinin activation: evidence for an ordered reaction mechanism for the tyrosyl protein sulfotransferase responsible for the peptide sulfation. Biochemical & Biophysical Research Communications 1991;181:989–996. [PubMed: 1764108]
20. Varin L, Ibrahim RK. Novel flavonol 3-sulfotransferase. Purification, kinetic properties, and partial amino acid sequence. Journal of Biological Chemistry 1992;267:1858–1863. [PubMed: 1309801]
21. Kim DH, Kim HS, Imamura L, Kobashi K. Kinetic studies on a sulfotransferase from Klebsiella K-36, a rat intestinal bacterium. Biological & Pharmaceutical Bulletin 1994;17:543–545. [PubMed: 8069266]

22. Gorokhov A, Perera L, Darden TA, Negishi M, Pedersen LC, Pedersen LG. Heparan sulfate biosynthesis: A theoretical study of the initial sulfation step by N-Deacetylase/N-sulfotransferase. Biophysical Journal 2000;79:2909–2917. [PubMed: 11106599]
23. Kakuta Y, Pedersen LG, Carter CW, Negishi M, Pedersen LC. Crystal structure of estrogen sulphotransferase. Nat Struct Biol 1997;4:904–908. [PubMed: 9360604]
24. Kakuta Y, Pedersen LC, Chae K, Song WC, Leblanc D, London R, Carter CW, Negishi M. Mouse steroid sulfotransferases: substrate specificity and preliminary X-ray crystallographic analysis. Biochemical Pharmacology 1998;55:313–317. [PubMed: 9484797]
25. Petrotchenko EV, Doerflein ME, Kakuta Y, Pedersen LC, Negishi M. Substrate gating confers steroid specificity to estrogen sulfotransferase. Journal of Biological Chemistry 1999;274:30019–30022. [PubMed: 10514486]
26. Pedersen LC, Petrotchenko E, Shevtsov S, Negishi M. Crystal structure of the human estrogen sulfotransferase-PAPS complex: Evidence for catalytic role of Ser137 in the sulfuryl transfer reaction. J Biol Chem 2002;277:17928–17932. [PubMed: 11884392]
27. Shevtsov S, Petrotchenko EV, Pedersen LC, Negishi M. Crystallographic analysis of a hydroxylated polychlorinated biphenyl (OH-PCB) bound to the catalytic estrogen binding site of human estrogen sulfotransferase. Environ Health Perspect 2003;111:884–888. [PubMed: 12782487]
28. Moon AF, Edavettal SC, Krahn JM, Munoz EM, Negishi M, Linhardt RJ, Liu J, Pedersen LC. Structural analysis of the sulfotransferase (3-o-sulfotransferase isoform 3) involved in the biosynthesis of an entry receptor for herpes simplex virus 1. J Biol Chem 2004;279:45185–45193. [PubMed: 15304505]
29. Edavettal SC, Lee KA, Negishi M, Linhardt RJ, Liu J, Pedersen LC. Crystal structure and mutational analysis of heparan sulfate 3-O-sulfotransferase Isoform 1. J Biol Chem 2004;279:25789–25797. [PubMed: 15060080]
30. Lee KA, Fuda H, Lee YC, Negishi M, Strott CA, Pedersen LC. Crystal structure of human cholesterol sulfotransferase (SULT2B1b) in the presence of pregnenolone and 3′-phosphoadenosine 5′-phosphate. Rationale for specificity differences between prototypical SULT2A1 and the SULT2BG1 isoforms. J Biol Chem 2003;278:44593–44599. [PubMed: 12923182]Epub 42003 Aug 44514
31. Barnes S, Waldrop R, Crenshaw J, King RJ, Taylor KB. Evidence for an ordered reaction mechanism for bile salt: 3′phosphoadenosine-5′-phosphosulfate: sulfotransferase from rhesus monkey liver that catalyzes the sulfation of the hepatotoxin glycolithocholate. Journal of Lipid Research 1986;27:1111–1123. [PubMed: 3470420]
32. Pi N, Yu Y, Mougous JD, Leary JA. Observation of a hybrid random ping-pong mechanism of catalysis for NodST: a mass spectrometry approach. Protein Sci 2004;13:903–912. [PubMed: 15044725]
33. Kim DH, Kobashi K. Kinetic studies on a novel sulfotransferase from Eubacterium A-44, a human intestinal bacterium. Journal of Biochemistry 1991;109:45–48. [PubMed: 1901853]
34. Lee NS, Kim BT, Kim DH, Kobashi K. Purification and reaction mechanism of arylsulfate sulfotransferase from Haemophilus K-12, a mouse intestinal bacterium. Journal of Biochemistry 1995;118:796–801. [PubMed: 8576095]
35. Kwon AR, Yun HJ, Choi EC. Kinetic mechanism and identification of the active site tyrosine residue in Enterobacter amnigenus arylsulfate sulfotransferase. Biochem Biophys Res Commun 2001;285:526–529. [PubMed: 11444874]
36. Pi N, Hoang MB, Gao H, Mougous JD, Bertozzi CR, Leary JA. Kinetic measurements and mechanism determination of Stf0 sulfotransferase using mass spectrometry. Anal Biochem 2005;341:94–104. [PubMed: 15866533]
37. Cook, PF.; Cleland, WW. Enzyme kinetics and mechanism. Garland Science; 2007.
38. Leskovac, V. Comprehensive Enzyme Kinetics. Springer; 2003.
39. Purich DL, Allison RD. Isotope exchange methods for elucidating enzymic catalysis. Methods Enzymol 1980;64:1–46. [PubMed: 6990185]
40. Chen G, Battaglia E, Senay C, Falany CN, Radominska-Pandya A. Photoaffinity labeling probe for the substrate binding site of human phenol sulfotransferase (SULT1A1): 7-azido-4-methylcoumarin. Protein Science 1999;8:2151–2157. [PubMed: 10548061]

41. Chen G, Rabjohn PA, York JL, Wooldridge C, Zhang D, Falany CN, Radominska-Pandya A. Carboxyl residues in the active site of human phenol sulfotransferase (SULT1A1). Biochemistry 2000;39:16000–16007. [PubMed: 11123927]

42. Falany CN, Krasnykh V, Falany JL. Bacterial expression and characterization of a cDNA for human liver estrogen sulfotransferase. Journal of Steroid Biochemistry & Molecular Biology 1995;52:529–539. [PubMed: 7779757]

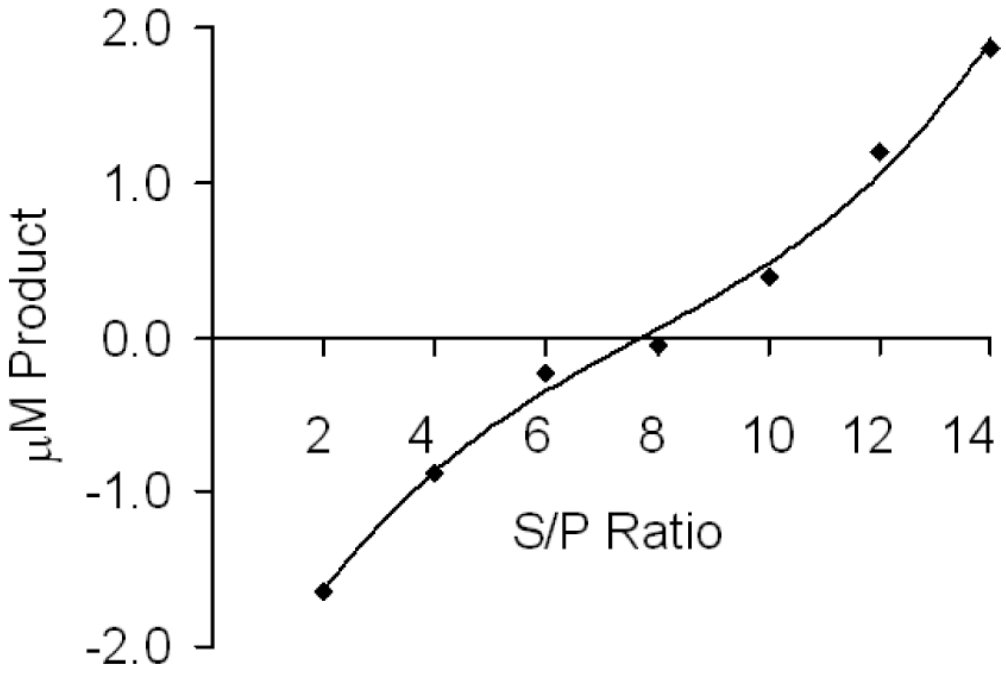

Figure 1.

Estimation of K_{eq} by varying S/P and measuring the change in radiolabeled reactant. The reaction was equilibrated using $[(^{14}C)1\text{-naphthol}]_0 = 20 \propto M$, and $[PAPS]_0 = 10 \propto M$, and then adding S/P (cold) in different ratios to the reaction mixture. The change in product concentration was monitored using scintillation counting.

Figure 2A

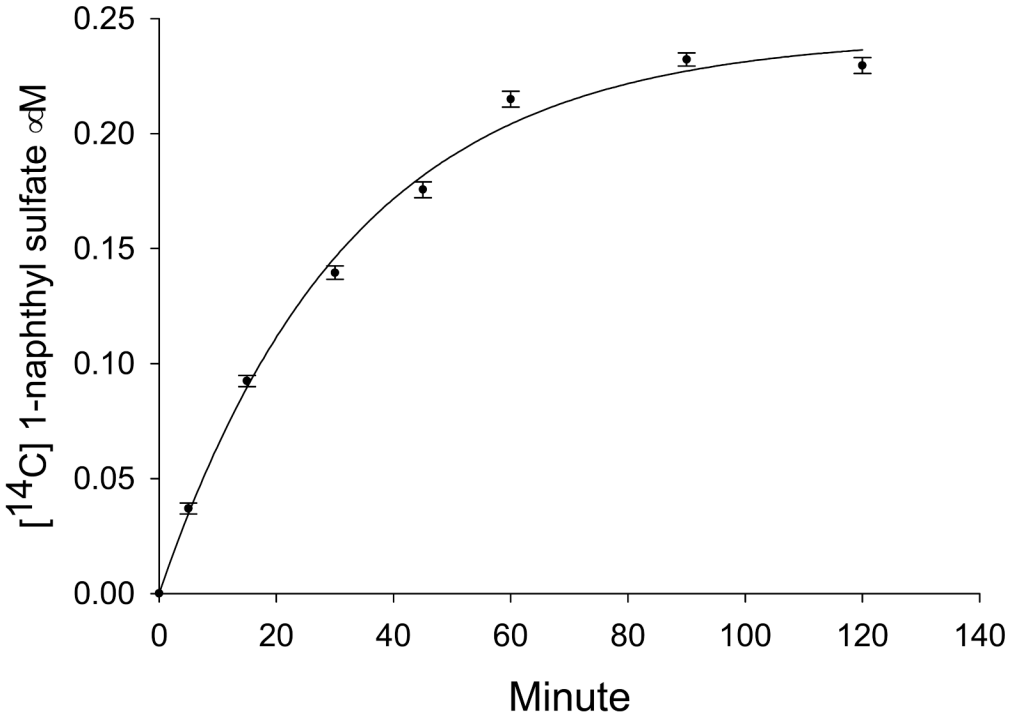

Figure 2B

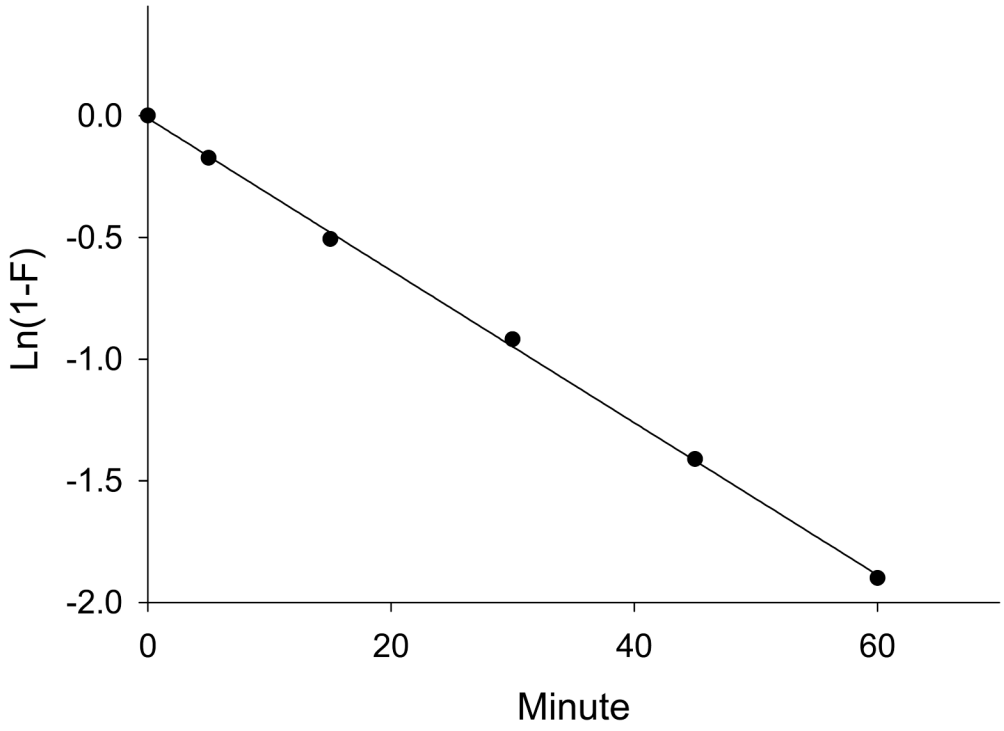

Figure 2.

A. Time course for the 1-naphthol to 1-naphthyl sulfate exchange reaction monitoring the appearance of [^{14}C]-1-naphthyl sulfate. Concentrations of PAPS, PAP, 1-naphthol, 1-naphtyl sulfate are 20 ∝M, 4 ∝M, 50 ∝M, and 5 ∝M, respectively, consistent with the equilibrium constant. The concentration of added [^{14}C]-1-naphtol pulse is 0.5 ∝M. Each reaction included 7.5 ∝g SULT1A1 in 50 ∝L phosphate buffer (final concentration: 50 mM, pH 6.2) at 37°C. The curve fitting was done using Enzyme Kinetics Module 1.2 (SigmaPlot). B. First order plot of the data in A as $\ln(1 - f)$ vs. time.

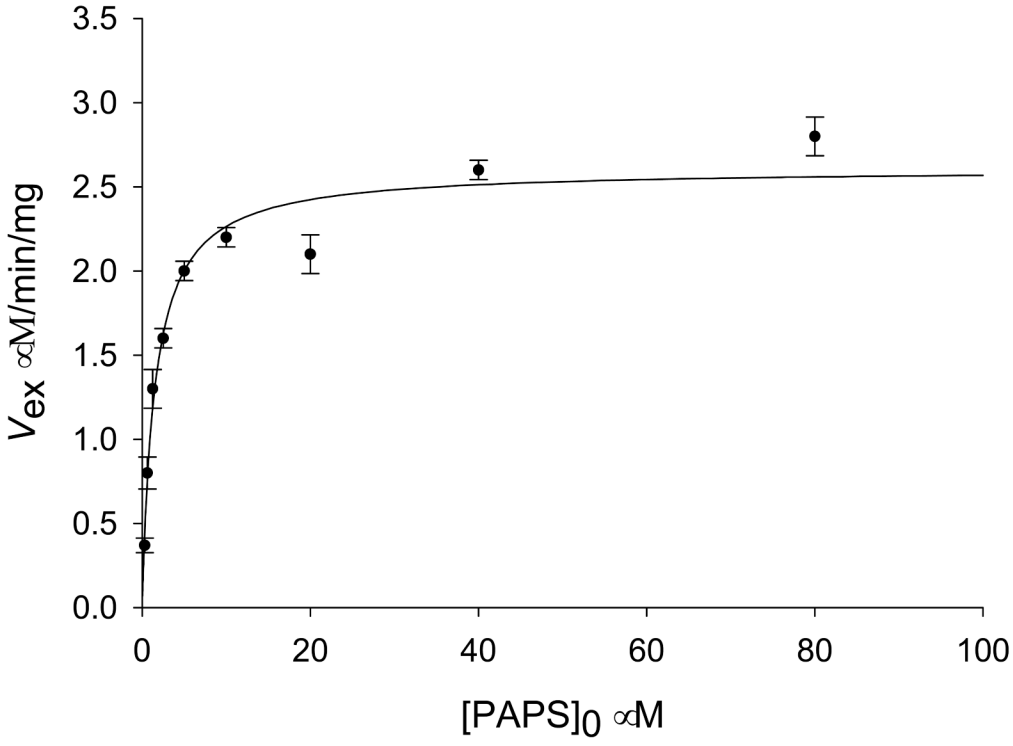

Figure 3.
Initial rates of [^{14}C]S ⇋ [^{14}C]P isotopic exchange versus $[PAPS]_0/[PAP]_0$ ratios. Concentrations of 1-naphthol, 1-naphtyl sulfate are 50 ∝M, and 5 ∝M, respectively. Concentration of added [^{14}C]1-naphtol pulse is 0.5 ∝M; 7.5 ∝g SULT1A1 in 50 ∝l phosphate buffer (final concentration: 50 mM, pH 6.2) at 37°C. The curve fitting was done using Enzyme Kinetics Module 1.2 (SigmaPlot).

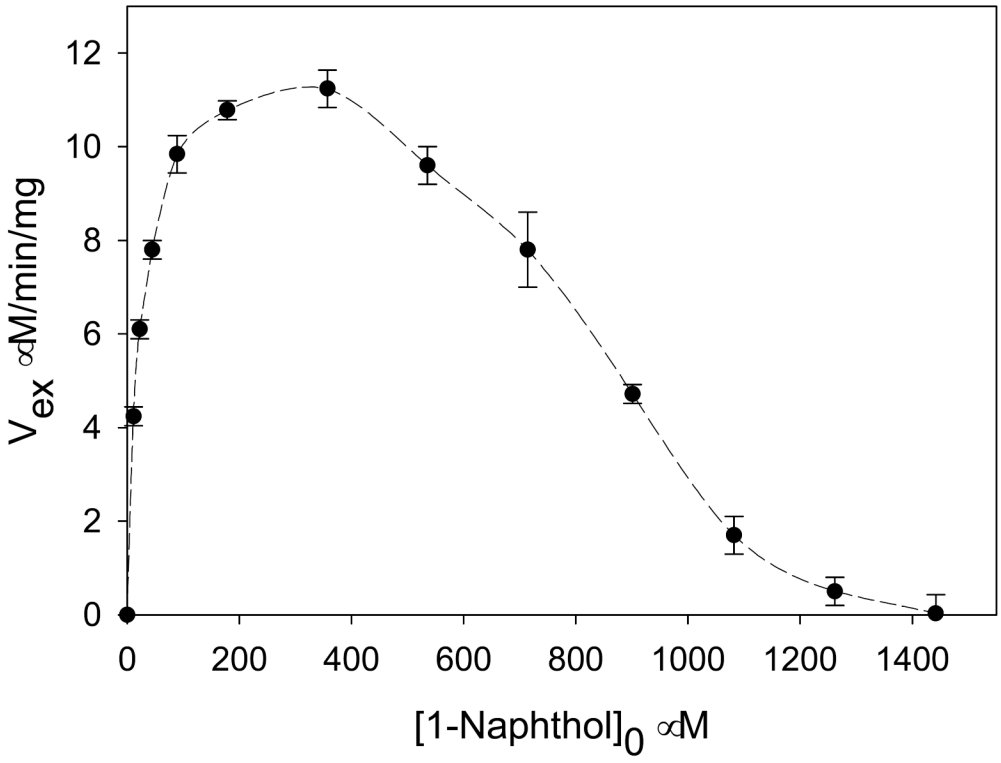

Figure 4.
Rates of [^{35}S]PAPS ⇋ [^{35}S]P isotopic exchange versus $[S]_0/[P]0$ ratios. Concentrations of PAPS and PAP are 10 ∝M and 2 ∝M, respectively. Concentration of added [^{35}S]PAPS pulse is 0.05 ∝M; 7.5 ∝g SULT1A1 in 50 ∝l phosphate buffer (final concentration: 50 mM, pH 6.2) at 37°C.

Scheme 1.
SULT- catalyzed reactions.

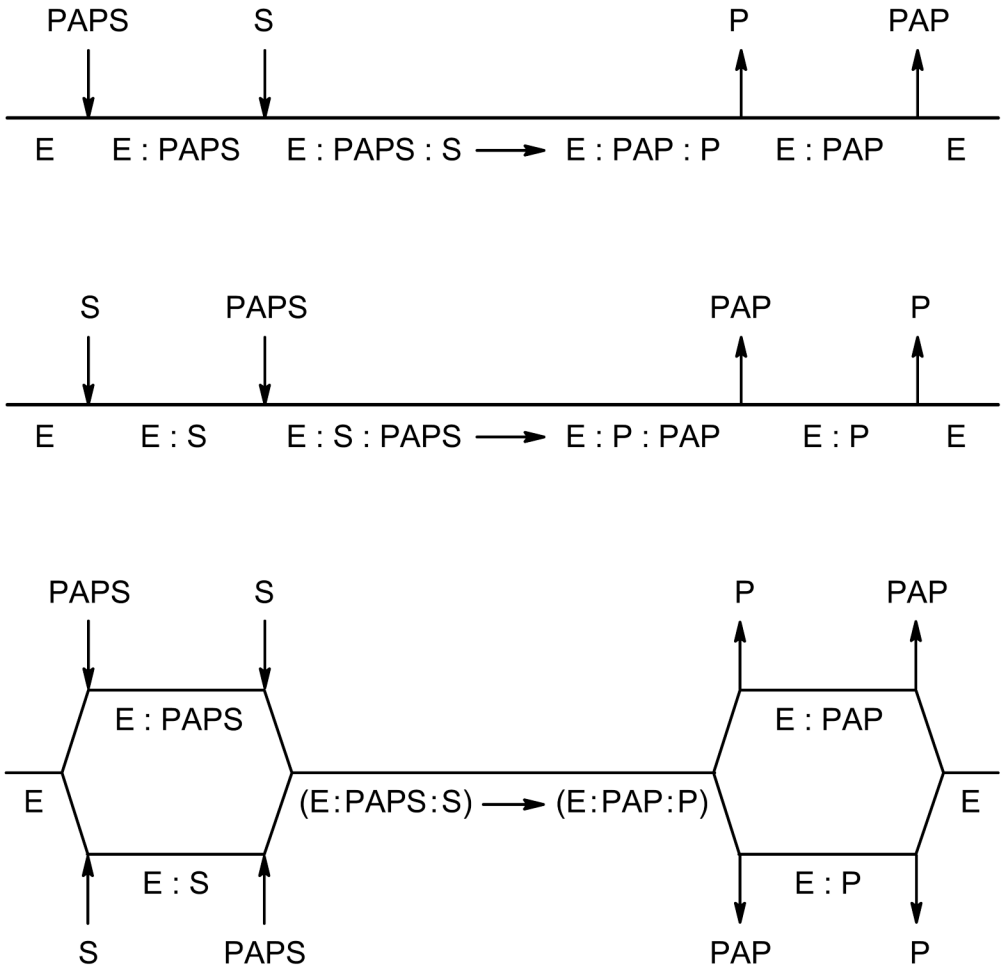

Scheme 2.
Possible mechanisms for SULT-catalyzed reactions.

Table 1

K_e values determined by using various initial concentrations of PAPS and [^{14}C]1-naphthol.

$[PAPS]_0$, ∝M	$[(^{14}C)1\text{-naphthol}]_0$, ∝M	K_e
2	2	0.021 ± 0.004
2	4	0.019 ± 0.002
2	8	0.022 ± 0.003
10	10	0.023 ± 0.003
10	20	0.021 ± 0.003
10	50	0.023 ± 0.002
80	20	0.019 ± 0.002
80	40	0.024 ± 0.002
80	50	0.021 ± 0.003

Table 2

K_e values determined by [^{35}S]PAPS and [^{35}S]1-naphthyl sulfate.

[(^{35}S)PAPS]$_0$, ∝M	[1-naphthol]$_0$, ∝M	K_e
10	50	0.04 ± 0.01
10	100	0.031 ± 0.008